

Temperature Dependence of Ion Mobility of Carbon Cluster Cations: Intermediate Region Connecting Low- and High-Field Conditions

Kiichirou Koyasu, Tomohiro Ohtaki, and Fuminori Misaizu*

Department of Chemistry, Graduate School of Science, Tohoku University, Aramaki, Aoba-ku, Sendai 980-8578

Received August 9, 2011; E-mail: misaizu@m.tohoku.ac.jp

Effective temperature (T_{eff}) dependences of reduced mobilities and collision cross section of small carbon cluster cations, C_n^+ ($n = 6$–25), were investigated by using a drift cell with temperatures of 170–300 K coupled with a reflectron time-of-flight mass spectrometer. We have measured ion mobility within $E/N = 16$–28 Td, values of which are slightly higher than the general experimental value at low-field conditions. Thus, our conditions should correspond to medium field strength between low- and high-field conditions. Under the present conditions, collision cross section was found to be proportional to $T_{\mathrm{eff}}^{-0.1} - T_{\mathrm{eff}}^{-0.2}$. The power in the temperature dependence was slightly closer to zero than results obtained previously (A. A. Shvartsburg, G. C. Schatz, M. F. Jarrold, *J. Chem. Phys.*, **1998**, *108*, 2416). This difference is probably due to E/N, resulting in the difference of relative kinetic energy between C_n^+ and buffer gas atoms, in spite of the same T_{eff} region. The result showed that the hard-sphere model is more applicable in the present conditions.

Clusters have specific reactivities depending on their sizes and structures. They can be regarded as model systems for catalytic reactions on solid surfaces,[1] since reactive sites on catalysts also have specific structures. However, structures of clusters are usually difficult to determine in spite of their importance. One of the ways to know the structure is a combination of experimental results and theoretical predictions. Electronic[2] and vibrational spectroscopies[3] are usually used as experimental methods. In addition, ion mobility measurement is another technique to obtain information about the geometric structures from collision cross sections.

Ion mobility spectrometry is a powerful technique also for separation of ion isomers directly in gas phase.[4] Recently the spectrometry has been utilized in wide a range of fields including applications, such as poisonous gas or explosive gas detection in military and security.[5] This method has also long been adopted to cluster science. There is a lot of pioneering work on ion mobility spectrometry of clusters both experimentally and theoretically.[6–18] Carbon clusters have been extensively investigated by this method since the structural variations are based on sp and sp^2 hybridization as well as sp^3.[6–9,11,12,15] The hybridizations lead to linear, planar, and 3-dimensional structures. Carbon clusters are also known to have another allotrope, fullerene.

Ion mobility, K, is defined as $K = v_d/E$, in which v_d is drift velocity and E is electric field applied in a drift cell. Here v_d increases with increasing E and with decreasing number density of buffer gas, N. Thus the ratio E/N is an important parameter to control v_d experimentally, and separation conditions of isomers depend on this parameter. In general, two extreme conditions have been discussed so far;[19] one is low-field and the other is high-field. In the low-field condition, ion mobility can be modeled based on kinetic theory as shown below. In this limit, typical magnitudes of E/N were 1–2 Td in plasma chromatography,[19] and in other experiments on carbon clusters E/N were 1.5–10 Td,[9–11] where Td is the unit corresponding to 10^{-17} V cm^2. On the other hand, in the high-field condition, kinetic energy of ions is so large that ion mobility shows nonlinear dependence on E/N.[20]

We have used slightly higher values of E/N than the low-field conditions to observe isomer-specific dissociation reactions after isomer separation by ion mobility spectrometry.[21] For applications of spectroscopic methods to cluster ions after isomer separations, strong ion beam intensity is required. To increase the ion intensity, we have adopted a larger orifice and a modest pressure (≈0.8–1.0 Torr). In order to separate different isomers for the following spectroscopic application, the number density N and thus the collision frequency inside of the cell were increased by lowering the temperature of the drift cell to ≈170 K. Therefore, information on temperature dependence of ion mobility is indispensable for determining proper conditions for such experiments.

Ion mobility can be modeled as a function of temperature based on kinetic theory under the low-field condition;

$$K = \frac{3e}{16N}\sqrt{\frac{2\pi}{k_{\mathrm{B}}T_{\mathrm{eff}}\mu}}\frac{1}{\Omega} \tag{1}$$

where e is the elementary charge, k_{B} is the Boltzmann constant, and μ is reduced mass. Ω is a collision integral or a collision cross section, which is in general a function of temperature. Assuming that Ω is independent of temperature, it is regarded as a collision cross section in the hard-sphere model. T_{eff} represents the effective temperature defined as

$$T_{\mathrm{eff}} = T + \frac{Mv_d^2}{3k_{\mathrm{B}}} \tag{2}$$

where T is the drift cell temperature and M is the mass of the buffer gas. The effective temperature includes internal energy

Published on the web November 29, 2011; doi:10.1246/bcsj.20110238

increase of the ions by collision with the buffer gas atoms. In the low-field condition, the second term of the right side of eq 2 is so low that T_{eff} can be approximated with T.

Ion mobility is customarily discussed using the reduced mobility, K_0, in which the number density at the measurement condition is exchanged with that at the standard condition ($T_0 = 273.15\,\mathrm{K}$ and $p_0 = 760\,\mathrm{Torr}$), N_0;[22]

$$K_0 = \frac{N}{N_0} K = \frac{T_0}{T} \frac{p}{p_0} K \tag{3}$$

Thus eq 1 can be written as

$$K_0 = \frac{3e}{16} \sqrt{\frac{2\pi}{k_{\mathrm{B}}\mu}} \frac{1}{N_0} \sqrt{\frac{1}{T_{\mathrm{eff}}}} \frac{1}{\Omega} \tag{4}$$

Because Ω is a function of temperature as noted above, it can be written as $\Omega(T_{\mathrm{eff}})$. Therefore K_0 is dependent on temperature through the term ${T_{\mathrm{eff}}}^{-0.5}\Omega(T_{\mathrm{eff}})^{-1}$.

The problem of how K_0 varies with temperature has been actively discussed.[9–11,23–26] Previous studies showed that the mobility changes with temperature due to hydration, protonation, or clustering reactions in the drift cell.[24,25] A functional form of $\Omega(T_{\mathrm{eff}})$ was also investigated in order to explain the observed temperature dependences of K_0.[9–11,26] It was one of the main reasons that the polarization model (Langevin model) is applicable to the experimental temperature dependence of $\Omega(T_{\mathrm{eff}})$ at extremely low temperature.[26] As for the cluster ion studies, dependence of K_0 upon temperature was investigated for small carbon clusters in some detail.[9–11] $\Omega(T_{\mathrm{eff}})$ was theoretically evaluated in those studies by trajectory calculations employing a realistic ion–He interaction potential using Lennard–Jones potential.

In this study, we have investigated the temperature dependence of ion mobilities of C_n^+ ($n = 6$–25), consisting of linear and cyclic isomers, using a drift cell (cooled by liquid nitrogen) combined with a reflectron time-of-flight mass spectrometer (TOFMS). The present experiment was done under medium-field conditions, $E/N = 16$–$28\,\mathrm{Td}$, and the effective temperature was varied in the range of 170–400 K. We have compared the T_{eff} dependence of $\Omega(T_{\mathrm{eff}})$ obtained from the measured K_0 with those based on Langevin and hard-sphere models. The results were also compared with those previously obtained by Bowers' group[10] and Jarrold's group.[9,11]

Experimental

Present experiments were performed using a home-built vacuum apparatus composed of a cluster ion source, an ion drift-tube cell, and a reflectron TOFMS.[27] Details of the experimental procedures will be reported elsewhere.[28] Here, we briefly describe the experimental setup and conditions for isomer separation in the drift cell. Carbon cluster ions were produced by a laser vaporization of graphite disk with the second harmonic of a Nd:YAG laser (532 nm). The produced cluster ions were introduced into the drift cell through an ion gate with a pulsed electric field ($600\,\mathrm{V\,cm^{-1}}$) at a given time, $t = t_0$. Isomers of the cluster ions were then separated at a temperature range between 170–300 K in the drift cell, in which the pressure of He buffer gas was 0.8 Torr and drift electric field was $7.2\,\mathrm{V\,cm^{-1}}$. The cell length was 10.05 cm. The separated isomer ions in the drift cell were introduced to the Wiley–McLaren acceleration region (acceleration energy of 1.3 kV) of the reflectron TOFMS. The acceleration timing of the ions, $t = t_0 + \Delta t$, was scanned to detect the time of each isomer ion reaching at the acceleration region after the injection to the drift tube. The time for passing through the drift cell, Δt, is denoted by "arrival time."

Because the ions produced in the source were initially separated by their mobility without mass separation, each ion bunch reaching the acceleration region of TOFMS consists of various ion species with similar cross section. The ion bunch was followed by mass analysis with the reflectron TOFMS. We thus obtained a series of TOF mass spectra sequentially by scanning the arrival time. The total intensities of ion peaks with the same mass were plotted as a function of arrival time, which we hereafter denote an arrival time distribution (ATD) plot. The peak of the ATD plot corresponds to the representative arrival time of a certain isomer of the ion.

The effective temperature of each isomer ion was calculated from eq 2 using the cell temperature and the ion drift velocity. The drift velocity was estimated from the representative arrival time. On the other hand, the temperature of the ion-drift cell can be lowered by a liquid nitrogen flow in a copper tube surrounding the cell. In this study, the effective temperature was controlled by tuning the cell temperature with a constant buffer gas pressure and a constant electric field applied in the cell.

Results and Discussion

Representative Arrival Time and Ion Mobility. In order to obtain the representative arrival times and ion mobilities of carbon cluster cations, C_n^+ ($n = 6$–25), we first measured a series of TOF mass spectra with changing the arrival times, Δt, at 170 K. Then we made a two-dimensional plot of ion intensities as functions of arrival time (measure of ion mobility) and their TOF (measure of cluster size), as shown in Figure 1. The results shown in the plot were generally consistent with the previous reports;[6] linear isomers were observed at $6 \le n \le 10$, while cyclic isomers were observed at $7 \le n \le 25$. The linear and cyclic isomers coexisted at $n = 7$–10.

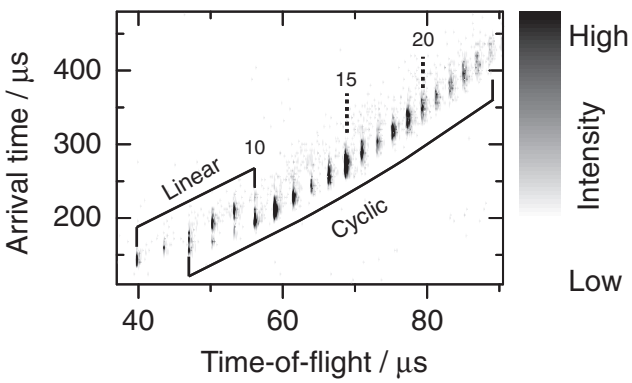

Figure 1. Two-dimensional contour plot of ion intensities of C_n^+ cluster cations ($n = 6$–25). The horizontal axis represents arrival times and vertical axis represents their TOF. The intensity of C_n^+ is shown by shading the contours according to the color bar on the right hand side. Numbers represent the cluster sizes, and size ranges for linear and cyclic isomers are indicated.

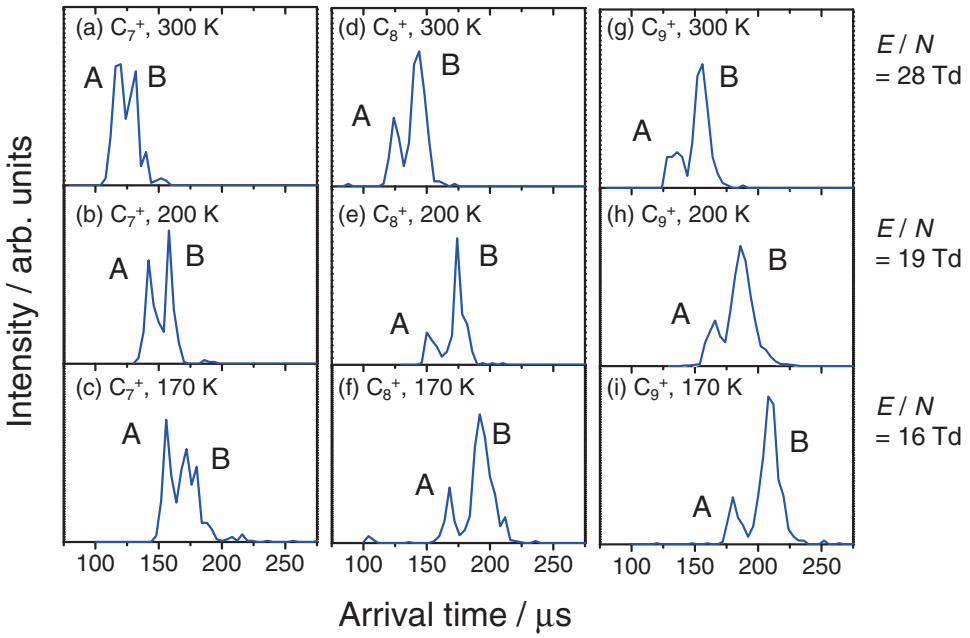

Figure 2. Arrival time distributions (ATDs) of C_n^+ ($n = 7$–9) measured at 170–300 K. The ratios of E/N are also shown. Peaks A and B correspond to cyclic and linear isomers, respectively.

From the series of TOF mass spectra measured, we also obtained an ATD plot for each carbon cluster ion. Figure 2 shows examples of ATD plots for C_n^+ with $n = 7$–9. The ATD of C_7 observed at 300 K, shown in Figure 2a, has two ion packets peaking at 116 μs (A) and at 132 μs (B). These two peaks correspond to cyclic (A) and linear (B) isomers. We also fulfilled the same measurements at cell temperatures of 250, 200, 190, and 170 K. As expected, the ATDs shifted to larger values with decreasing temperature. Drift velocities v_d of the isomer ions were calculated using the determined representative arrival times deduced from ATD plots. Arrival times and drift velocities of C_n^+ ($n = 7$–9) at the temperature of 170, 200, and 300 K corresponding to the peaks shown in Figure 2 are listed in Table 1. Ion mobilities of C_n^+ ($n = 6$–25) were then calculated by the equation of $K = v_d/E$. The reduced mobilities K_0 were also calculated by eq 3. We measured mobilities of the following cluster ion isomers; linear isomers of C_6^+–C_{10}^+ and ring isomers of C_7^+–C_{25}^+. Among these ions, reduced mobilities of linear C_6^+ (a), cyclic C_{10}^+ (b), linear C_{10}^+ (c), and cyclic C_{25}^+ (d) measured at various temperatures were plotted as a function of their effective temperature T_{eff} in Figure 3. These ions correspond to the smallest linear, the smallest cyclic, the largest linear, and the largest cyclic isomers in this study, respectively. As shown in this figure, the reduced mobilities of the four clusters decreased gradually with their effective temperature. This tendency was also observed for the other isomers of clusters investigated in this study.

Table 1. Arrival Times and Drift Velocities of C_n^+ ($n = 7$–9) at the Temperature of 170, 200, and 300 K Corresponding to the Peaks Shown in Figure 2

Temperature	Cluster		Arrival time/μs	Drift velocity/m s^{-1}
300	C_7^+	A	116	1006
		B	132	868
	C_8^+	A	124	941
		B	144	794
	C_9^+	A	132	884
		B	156	731
200	C_7^+	A	142	799
		B	158	710
	C_8^+	A	154	736
		B	178	626
	C_9^+	A	166	681
		B	186	600
170	C_7^+	A	156	720
		B	176	630
	C_8^+	A	168	668
		B	192	576
	C_9^+	A	180	681
		B	208	531

Previous Studies on Temperature Dependence of Reduced Mobility and Collision Cross Section. We will hereafter discuss temperature dependence of collision cross section, Ω, derived from reduced mobility. At first, temperature dependence of Ω is summarized for Langevin and hard-sphere models. Assuming that Ω is determined only by the radii of the ions and He atoms, Ω is independent of temperature in the hard-sphere approximation; $\Omega \propto T_{eff}^0$. On the other hand, considering the charge-induced dipole interaction between the ion and the neutral buffer gas, collision cross section is determined by the balance of the induced attractive force and a centrifugal force. The temperature dependence of Ω is then expressed as $\Omega \propto T_{eff}^{-0.5}$, in which Ω is called Langevin cross section.

Temperature dependences of K_0 was already investigated for the C_{60}^+ fullerene[9,10] and linear and cyclic isomers of C_n^+ ($n = 5$–40).[11] The measurements were done under different conditions from the present experiment; the low-field condition with $E/N = 1.5$–10 Td. The results were all compared with the

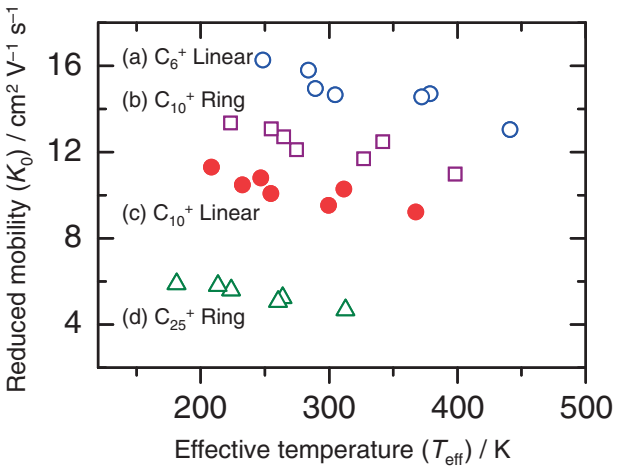

Figure 3. Reduced mobilities K_0 of linear C_6^+ (open circle, a), cyclic C_{10}^+ (open square, b), linear C_{10}^+ (filled circle, c), and cyclic C_{25}^+ (open triangle, d) measured at various temperatures are plotted as a function of T_{eff}.

K_0 values obtained from their Ω determined by trajectory calculations including a C–He potential as long-range interactions. The calculated K_0 agreed with the experimental results rather than that using hard-sphere approximation.[9,11] From their results for C_{60}^+ and C_{5-10}^+ with linear structures, one can deduce the temperature dependence of Ω are proportional to $T_{eff}^{-0.2} - T_{eff}^{-0.3}$ within the range of $T_{eff} = 150$–400 K. The power is a middle value between those obtained from the Langevin cross section and those from the hard-sphere approximation.

Present Temperature Dependence of the Reduced Mobility and the Cross Section. In the analysis deducing temperature dependence of the reduced mobilities, we assumed an equation for K_0 to be $K_0 = C \times (T_{eff})^{\alpha}$ from eq 4. Typical plots of reduced mobility with logarithmic scale against T_{eff} are shown in Figure 4. The slope α was determined to be ca. −0.3 to −0.4, that is $K_0 \propto T_{eff}^{-0.3} - T_{eff}^{-0.4}$, by least-squares fittings for most of the species investigated here, linear $n = 6$–10 and cyclic $n = 7$–25. Because Ω should be proportional to $T_{eff}^{-0.5-\alpha}$ from eq 4, temperature dependence of Ω is written as $\Omega \propto T_{eff}^{-0.1} - T_{eff}^{-0.2}$ from our measurements. The powers obtained here are plotted in Figure 5 along with those of the previous results[11] and the models noted in the above section in order to compare with each other. Averaged α values of the present and the previous results were determined to be −0.16 and −0.23, respectively. Our temperature dependence of Ω is close to the relation of the result under low-field condition. Both of the powers, $-0.5 - \alpha$, are intermediate between zero (the model of the hard-sphere approximation) and −0.5 (that of the Langevin cross section). However, the powers obtained in the present study show less temperature dependence than those in Refs. 9–11. At present we have no clear reason for this difference. However, it is probably due to the fact that larger E/N was used in our experiment than the previous studies, although the range of T_{eff} was the same. Because E/N and the resulting collision energy range in our experiment were larger than the previous studies, contribution of the long-range attractive force in the cross section is weakened in this study.

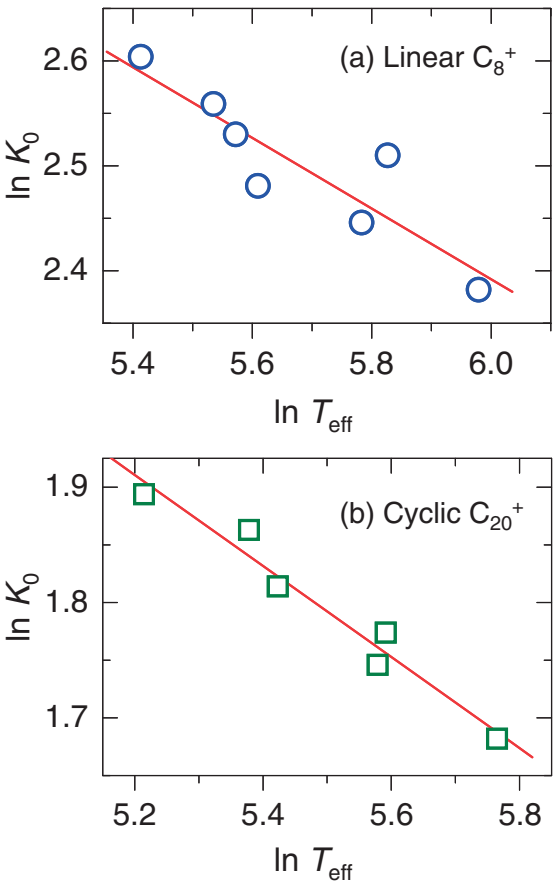

Figure 4. Reduced mobility plots of linear isomer of C_8^+ (a) and cyclic isomer of C_{20}^+ (b) vs. T_{eff} with logarithmic scales. The lines represent the results of least-squares fittings.

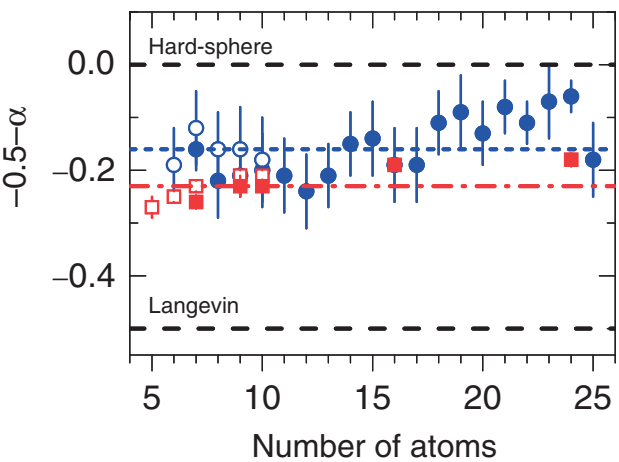

Figure 5. Plots of the power $(-0.5 - \alpha)$ in the T_{eff} dependence of the cross section for C_n^+ ($n = 6$–25). Open and filled circles represent data for linear and cyclic isomers of the present study. Open and filled squares represent data for linear and cyclic isomers measured in Ref. 11. Lines of the averaged values are also shown. The dashed line at $(-0.5 - \alpha) = 0$ and −0.5 represent the hard-sphere and the Langevin cross sections.

Therefore the cross section may be determined more by the interatomic repulsive interaction, and thus it may approach the hard-sphere cross section. It should be also noted that the power gradually approaches zero with increasing cluster size of C_n^+ in Figure 5. Although this tendency cannot be explained at present again, it appears to be commonly observed for the present and for the previous experiments.

Conclusion

Effective temperature dependences of the reduced mobilities K_0 and Ω of small carbon cluster cations, C_n^+ ($n = 6$–25), were investigated using the combination of the reflectron TOFMS and the drift cell with the T_{eff} range of 170–400 K. Under the experimental condition of $E/N = 16$–28 Td corresponding to a medium-field condition, Ω was found to be proportional to $T_{\text{eff}}^{-0.1} - T_{\text{eff}}^{-0.2}$. To discuss the present results, three types of temperature dependence of Ω are summarized as follows;

(A) For the hard-sphere approximation, Ω is determined only by the sum of radii of an ion and a buffer gas without any attractive/repulsive force; $\Omega \propto T_{\text{eff}}^{0}$.

(B) Ω within the Langevin cross section is determined by the balance between the charge-induced dipole attraction and a centrifugal repulsion, which is effective at long distance, especially for a low collision energy obtained under the low-field condition. As a result, $\Omega \propto T_{\text{eff}}^{-0.5}$.

(C) For the theoretical model discussed in Refs. 9–11, Ω is described by including a molecular attractive potential between the ion and He buffer gas atom, which is also effective as a long-range interaction. Their experimental results can be written as $\Omega \propto T_{\text{eff}}^{-0.2} - T_{\text{eff}}^{-0.3}$.

The power in the dependence of Ω determined by our study was smaller than the results obtained previously (C). The difference is probably due to that of E/N, resulting in the difference of relative kinetic energy between C_n^+ and buffer gas atoms, although the same T_{eff} region. This indicates that the present condition is approaching that suitable for the hard-sphere model (A) rather than the Langevin cross section (B).

This work was supported by Mitsubishi Foundation, Kurata Foundation, The Salt Science Foundation (Nos. 0508, 0616, and 0710), Yamada Science Foundation, Sumitomo Foundation, and also in part by a Grant-in-Aid for Scientific Research from the Japan Society for the Promotion of Science (JSPS).

References

1 P. B. Armentrout, *Annu. Rev. Phys. Chem.* **2001**, *52*, 423.

2 For example: W.-J. Chen, H.-J. Zhai, Y.-F. Zhang, X. Huang, L.-S. Wang, *J. Phys. Chem. A* **2010**, *114*, 5958.

3 For example: A. N. Alexandrova, A. I. Boldyrev, X. Li, H. W. Sarkas, J. H. Hendricks, S. T. Arnold, K. H. Bowen, *J. Chem. Phys.* **2011**, *134*, 044322.

4 G. A. Eiceman, Z. Karpas, *Ion Mobility Spectrometry*, Taylor & Francis, London, **2004**.

5 As review articles; for example: C. S. Creaser, J. R. Griffiths, C. J. Bramwell, S. Noreen, C. A. Hill, C. L. P. Thomas, *Analyst* **2004**, *129*, 984, and references therein.

6 G. von Helden, M.-T. Hsu, N. Gotts, M. T. Bowers, *J. Phys. Chem.* **1993**, *97*, 8182.

7 A. A. Shvartsburg, M. F. Jarrold, *Chem. Phys. Lett.* **1996**, *261*, 86.

8 M. F. Mesleh, J. M. Hunter, A. A. Shvartsburg, G. C. Schatz, M. F. Jarrold, *J. Phys. Chem. A* **1997**, *101*, 968.

9 M. F. Mesleh, J. M. Hunter, A. A. Shvartsburg, G. C. Schatz, M. F. Jarrold, *J. Phys. Chem.* **1996**, *100*, 16082.

10 T. Wyttenbach, G. von Helden, J. J. Batka, Jr., D. Carlat, M. T. Bowers, *J. Am. Soc. Mass Spectrom.* **1997**, *8*, 275.

11 A. A. Shvartsburg, G. C. Schatz, M. F. Jarrold, *J. Chem. Phys.* **1998**, *108*, 2416.

12 D. E. Clemmer, M. F. Jarrold, *J. Mass Spectrom.* **1997**, *32*, 577.

13 A. A. Shvartsburg, M. F. Jarrold, *Phys. Rev. A* **1999**, *60*, 1235.

14 A. A. Shvartsburg, B. Liu, M. F. Jarrold, K.-M. Ho, *J. Chem. Phys.* **2000**, *112*, 4517.

15 A. A. Shvartsburg, B. Liu, K. W. M. Siu, K.-M. Ho, *J. Phys. Chem. A* **2000**, *104*, 6152.

16 F. Furche, R. Ahlrichs, P. Weis, C. Jacob, S. Gilb, T. Bierweiler, M. M. Kappes, *J. Chem. Phys.* **2002**, *117*, 6982.

17 P. Weis, O. Welz, E. Vollmer, M. M. Kappes, *J. Chem. Phys.* **2004**, *120*, 677.

18 E. Oger, N. R. M. Crawford, R. Kelting, P. Weis, M. M. Kappes, R. Ahlrichs, *Angew. Chem., Int. Ed.* **2007**, *46*, 8503.

19 H. E. Revercomb, E. A. Mason, *Anal. Chem.* **1975**, *47*, 970.

20 E. G. Nazarov, S. L. Coy, E. V. Krylov, R. A. Miller, G. A. Eiceman, *Anal. Chem.* **2006**, *78*, 7697.

21 F. Misaizu, N. Hori, H. Tanaka, K. Komatsu, A. Furuya, K. Ohno, *Eur. Phys. J. D* **2009**, *52*, 59.

22 E. A. Mason, E. W. MacDaniel, *Transport Properties of Ions in Gases*, Wiley, NY, **1988**.

23 a) F. W. Karasek, S. H. Kim, S. Rokushika, *Anal. Chem.* **1978**, *50*, 2013. b) D. M. Lubman, *Anal. Chem.* **1984**, *56*, 1298.

24 a) G. A. Eiceman, E. G. Nazarov, J. E. Rodriguez, J. F. Bergloff, *Int. J. Ion Mobility Spectrom.* **1998**, *1*, 28. b) R. G. Ewing, G. A. Eiceman, J. A. Stone, *Int. J. Mass Spectrom.* **1999**, *193*, 57.

25 a) M. Tabrizchi, *Appl. Spectrosc.* **2001**, *55*, 1653. b) M. Tabrizchi, *Talanta* **2004**, *62*, 65. c) M. Tabrizchi, F. Rouholahnejad, *J. Phys. D: Appl. Phys.* **2005**, *38*, 857.

26 K. Ohtsuki, M. Hananoe, M. Matsuzawa, *Phys. Rev. Lett.* **2005**, *95*, 213201, and references therein.

27 K. Ohshimo, F. Misaizu, K. Ohno, *J. Chem. Phys.* **2002**, *117*, 5209.

28 K. Koyasu, T. Ohtaki, F. Misaizu, to be submitted.